

Hydroxy-1,2,5-oxadiazolyl moiety as bioisoster of the carboxy function. A computational study on γ -aminobutyric acid (GABA) related compounds

Paolo Tosco · Marco L. Lolli

Received: 3 September 2007 / Accepted: 9 January 2008 / Published online: 5 February 2008
© Springer-Verlag 2008

Abstract Recently, our research group has proposed the hydroxyfurazanyl (4-hydroxy-1,2,5-oxadiazole-3-yl) moiety as a new non-classical isoster of the carboxy function in the design of γ -aminobutyric acid (GABA) analogues. Some compounds showed significant activity at the GABA_A receptor, representing the only examples of pentatomic heterocycles bearing an ω -aminoalkyl flexible side chain in the position vicinal to the hydroxy group displaying agonist activity at this receptor subtype. In this work, an *ab initio* analysis of the structural and electronic features of furazan-3-ol is presented, in order to provide a theoretical basis to the claimed bioisosterism with the carboxy function. An *ab initio* conformational study with the C-PCM implicit solvent model was carried out to elucidate the reasons of the peculiar behaviour of the furazan models. Alongside, another conformational search through molecular dynamics in explicit solvent was accomplished, in order to validate the first method. The electronic features of the 4-hydroxy-1,2,5-oxadiazole-3-yl substructure seem to account for a marked stabilising effect of the putative bioactive conformation at the GABA_A receptor subtype. The 1,2,5-thiadiazole analogue, which shares the same conformational preference of its oxygenated counterpart, was identified as a potential candidate for synthesis and pharmacological testing.

Keywords Carboxyl group isoster · GABA_A receptor · 1, 2, 5-oxadiazole · Furazan

Introduction

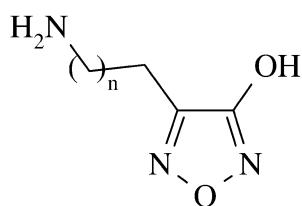
Isosteric replacement of functional groups is one of the classical pharmacomodulation approaches used in medicinal chemistry to improve the safety and activity profile of a lead compound [1]. When the replacement results in compounds sharing with the lead similar physicochemical and biological properties, then the groups are called bioisosters [2, 3]. Several examples of bioisosteric replacements are known in the literature; in particular, the carboxyl group has been successfully substituted by hetero- and carbocycles such as tetrazole, 3-hydroxyisoxazole, 3-hydroxyisothiazole, 3-hydroxy-1,2,5-thiadiazole and 3-cyclobutene-1,2-dione. These ring systems have been widely employed in the design of centrally active amino acid mimetics. Recently, the hydroxyfurazanyl (4-hydroxy-1,2,5-oxadiazole-3-yl) moiety has been proposed by our research group as a new non-classical isoster of the carboxyl group [4, 5]. When this ring system was used in the design of a series of analogues of γ -aminobutyric acid (Fig. 1), indeed it proved to behave as a bioisoster of the carboxy function [5].

Derivatives **1** and **2** showed moderate activity on GABA_A receptor as partial agonists, while **3** was a weak ligand, with mainly antagonistic properties (Table 1). Larsen and co-workers have synthesised throughout the years a large number of GABA_A ligands, which allowed the elucidation of structure-activity relationships and the progressive refinement of a 3D-pharmacophore model [6]. This model provides a sound explanation of the activity profile of the isoxazolol models THIP (**4a**), 4-PIOL (**5a**),

Electronic supplementary material The online version of this article (doi:10.1007/s00894-008-0269-0) contains supplementary material, which is available to authorised users.

P. Tosco (✉) · M. L. Lolli
Dipartimento di Scienza e Tecnologia del Farmaco,
Università degli Studi di Torino,
Via Pietro Giuria 9,
I-10125 Torino, Italy
e-mail: paolo.tosco@unito.it

Fig. 1 4-(ω -aminoalkyl)-1,2,5-oxadiazole-3-ol analogues of GABA [5]



- 1** n = 1
2 n = 2
3 n = 3

muscimol (**6a**) (Fig. 2), as well as of their respective isothiazolol analogues **4b–6b**. While homologation of muscimol and expansion of the THIP piperidine ring afforded derivatives which retain GABA_A agonism (homomuscimol, **7** [7]; THAZ, **8** [8]), changing the position of the protonated nitrogen inside the ring (THPO, **9** [9]; THIA, **10** [8]) resulted in inactive compounds. Substitution at the ring position vicinal to the hydroxyl group is allowed when giving rise to fused systems (**4a–b**, **8**), while in open-chain ligands (4-methylmuscimol, **11**; AEMI, **12**; **13**) it is always accompanied by loss of affinity [6]. This pattern of substitution is tolerated only for derivatives of 4-PIOL and its sulphur congener (**5a–b**), for which a different binding mode, made possible by a conformational shift of an arginine residue in the receptor, has been proposed [10, 6]; notably, all such compounds behave as potent antagonists. To the best of our knowledge, **1** and **2** represent the only examples of pentatomic heterocycles bearing an ω -aminoalkyl flexible side chain in the position vicinal to the hydroxyl group displaying agonist activity at the GABA_A receptor.

In order to provide a theoretical basis to the claimed bioisosterism, in the present work structural and electronic features of furazan-3-ol **16** were compared with those of the carboxyl group present in acrylic acid **17** and of its isoxazol congener **18** (Table 2). Then, a conformational study was carried out to shed light on the peculiar behaviour of the furazan models **1–3**.

Table 1 Binding affinities at the GABA_A receptor [5]^a

Compd	[³ H]muscimol binding K_i (μ M)
GABA	0.049 (0.043, 0.056)
4a (THIP)	0.16
5a (4-PIOL)	9.1 (8.2, 10)
1	13 (11, 16)
2	27 (25, 30)
3	>100

^a Standard receptor binding on rat brain synaptic membranes, $n=3$. Mean and SEM were calculated assuming a normal distribution of the logarithm of the K_i values. Numbers in parentheses (min, max) indicate the antilog of the log of the mean \pm SEM of K_i .

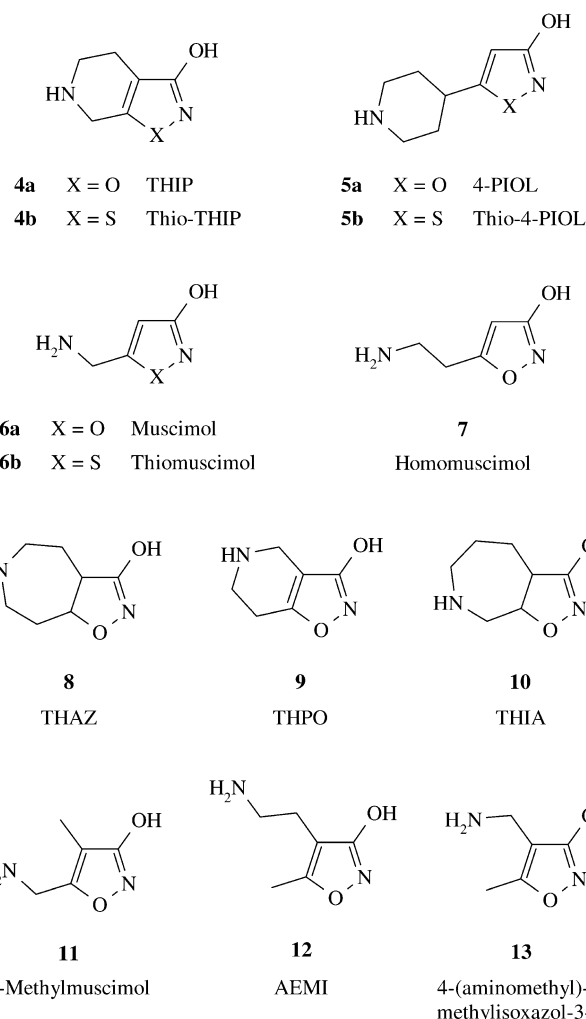


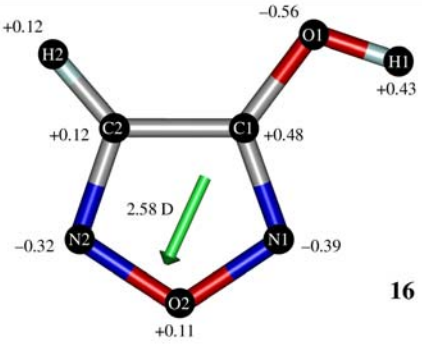
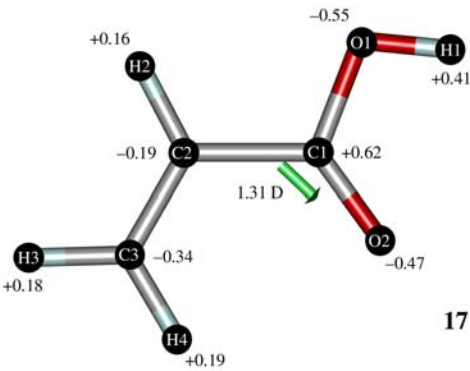
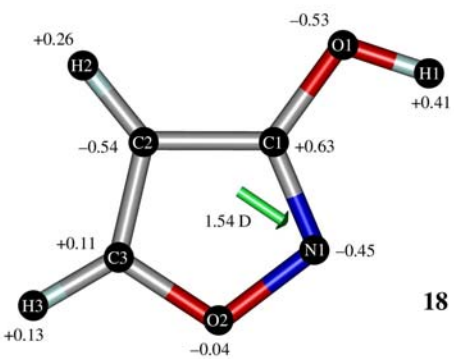
Fig. 2 GABA-like structures used as pharmacological tools or to elucidate structure-activity relationships

Methods

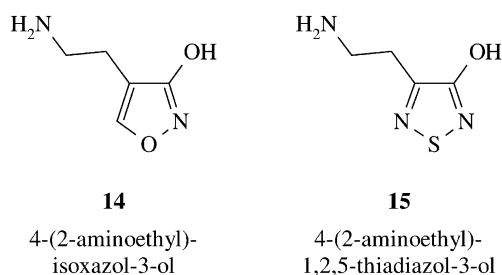
3D models of structures **16–18** (Table 2) were built from standard bond lengths and angles with the MOE modelling suite [11]. Their geometries were optimised in vacuum with C_s symmetry using *ab initio* methods at two different levels of theory, HF/6–31G(d) and MP2/6–311G(d,p), until the largest component of the gradient was less than $1 \cdot 10^{-5}$ Hartree Bohr⁻¹. The stationary points were characterised as true minima through vibrational analysis (no imaginary frequencies), then single-point calculations at the same level of theory were run in order to calculate the dipole moment and atom-centred ESP-derived charges (CHELPG method). All quantum-mechanical (QM) calculations were accomplished with the GAMESS-US package [12].

The 3D models of compounds **1–3**, **12**, **14**, **15** (Figs. 1, 2, 3) were built in their zwitterionic form from standard bond lengths and angles with MOE, while for compounds **4a–b** the crystallographic coordinates were available [13, 14]. All structures were optimised by a RHF/6–31G+(d) *ab initio*

Table 2 Calculated properties for compounds **16–18** (MP2/6–311G(d,p) level)

Compd ^a	Bond length (Å)	Bond angle (°)
 <p style="text-align: center;">16</p>	O(1)-H(1) 0.963	H(1)-O(1)-C(1) 107.64
	C(1)-O(1) 1.341	C(2)-C(1)-O(1) 126.66
	C(1)-N(1) 1.321	O(1)-C(1)-N(1) 123.90
	C(1)-C(2) 1.404	C(2)-C(1)-N(1) 109.43
	C(2)-H(2) 1.072	H(2)-C(2)-C(1) 130.29
	C(2)-N(2) 1.320	C(1)-C(2)-N(2) 108.69
	N(2)-O(2) 1.371	N(2)-C(2)-H(2) 121.02
	O(2)-N(1) 1.366	O(2)-N(2)-C(2) 105.24
		N(1)-O(2)-N(2) 111.75
		O(2)-N(1)-C(1) 104.89
 <p style="text-align: center;">17</p>	O(1)-H(1) 0.965	H(1)-O(1)-C(1) 105.39
	C(1)-O(1) 1.356	C(2)-C(1)-O(1) 111.05
	C(1)-O(2) 1.209	O(1)-C(1)-O(2) 123.01
	C(1)-C(2) 1.480	C(2)-C(1)-O(2) 125.94
	C(2)-H(2) 1.079	H(2)-C(2)-C(1) 117.60
	C(2)-C(3) 1.331	C(1)-C(2)-C(3) 119.83
	C(3)-H(3) 1.078	C(3)-C(2)-H(2) 122.57
	C(3)-H(4) 1.078	H(4)-C(3)-C(2) 121.42
		H(3)-C(3)-C(2) 119.65
		H(4)-C(3)-H(3) 118.93
 <p style="text-align: center;">18</p>	O(1)-H(1) 0.963	H(1)-O(1)-C(1) 106.98
	C(1)-O(1) 1.346	C(2)-C(1)-O(1) 125.50
	C(1)-N(1) 1.318	O(1)-C(1)-N(1) 121.89
	C(1)-C(2) 1.414	C(2)-C(1)-N(1) 112.61
	C(2)-H(2) 1.071	H(2)-C(2)-C(1) 128.52
	C(2)-C(3) 1.357	C(1)-C(2)-C(3) 102.78
	C(3)-H(3) 1.073	C(3)-C(2)-H(2) 128.70
	C(3)-O(2) 1.348	H(3)-C(3)-C(2) 133.54
	O(2)-N(1) 1.388	H(3)-C(3)-O(2) 115.72
		O(2)-C(3)-C(2) 110.74
	N(1)-O(2)-C(3) 108.64	
	O(2)-N(1)-C(1) 105.23	

^a CHELPG ESP-derived charges are reported near each atom; the green arrow represents the dipole moment vector (debye), pointing from the positive charge to the negative charge according to the convention followed in [21]. Figures were realised with the aid of the Gabedit package [22].

**Fig. 3** Isoxazole and 1,2,5-thiadiazole analogues of compound **1**

method setting the convergence criterion at $1 \cdot 10^{-4}$ Hartree Bohr⁻¹. Solvent effects were included using the polarisable continuum model C-PCM as implemented in GAMESS-US [15, 16].

On compounds **1**, **12**, **14**, **15** a systematic *ab initio* torsional search was carried out at the same level of theory used for the initial optimisation, by means of a two-step procedure. In the first step the two torsional angles C3-C4-C6-C7 (ϕ) and C4-C6-C7-C8 (ψ) (see Fig. 4) were varied

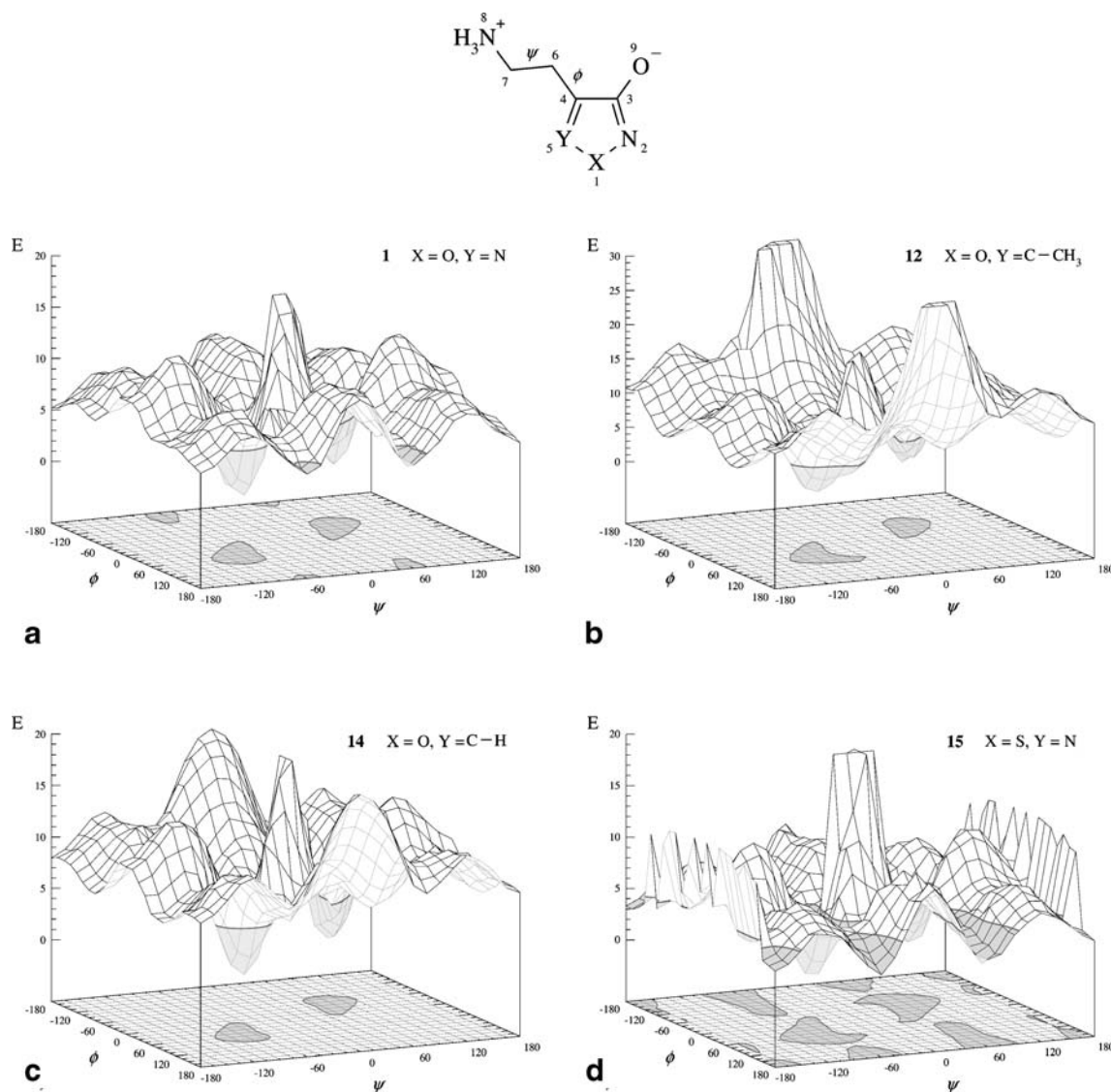


Fig. 4 Potential energy surfaces (PES) for compounds **1** (a), **12** (b), **14** (c), **15** (d). The potential energy (kcal mol⁻¹) is reported on the z axis vs the values of the dihedral angles ϕ , ψ (degrees). The energy values lying in a 5-kcal range from the global minimum have been

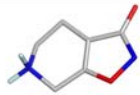

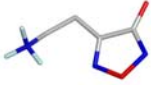


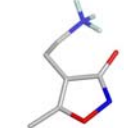
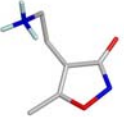
printed in grey on the 3D plot, while the corresponding ϕ , ψ ranges have been projected on the xy plane as grey areas. A 20-kcal cutoff has been adopted in the plot in favour of a more detailed rendering of the minima

over 15° increments, obtaining 576 possible conformers, coupled in 288 enantiomeric pairs since the planar pentatomic ring represents a plane of symmetry. The generated conformers underwent a constrained geometry optimisation freezing the two selected dihedrals at the initial values, while allowing the other internal coordinates free to relax, using a rather loose convergence criterion ($1 \cdot 10^{-3}$ Hartree Bohr⁻¹). This first step allowed thorough sampling of the potential energy surface (PES), in order to identify the range of the selected dihedrals giving rise to energetically accessible conformers in a 5-kcal range from the global minimum (Fig. 4).

On these conformers, a second unconstrained minimisation step was performed, this time with a tight convergence

criterion ($1 \cdot 10^{-5}$ Hartree Bohr⁻¹), which made most of the conformers found in the first step coalesce into the same local minima, thus reducing the number of possible minimum energy conformations to a few (see Tables 3, 4 and Fig. 5). Vibrational analysis allowed characterising the stationary points as true minima (no imaginary frequencies). Zero-point vibrational energies were scaled by a factor of 0.9153, while factors of 0.8945 and 0.9027 were adopted for the thermal contributions to enthalpy and entropy respectively, as suggested by Scott and Radom for the RHF/6-31G+(d) basis set [17]. The free energy of each conformer in aqueous solution was calculated according to Eq. 1 as the sum of E^{ele} (total electronic energy), E^{zp} (zero-point energy), G^{therm} (thermal contribution to enthalpy and entropy at

Table 3 Stable conformers of compounds **1**, **12** (*ab initio* C-PCM systematic search)

	Conformer	ΔG^a	ϕ^b	ψ^b	RMSD
THIP 4a		-	161.91	45.55	0.00 ^c
Compd 1		0.00	53.57	-75.75	1.32 ^c
		+3.18	170.61	63.98	0.23 ^c
		+3.31	-74.81	-67.27	0.73 ^c
		+4.80	69.35	-178.46	1.03 ^c
Compd 12		0.00	57.53	-75.33	1.33 ^c
		+3.54	-68.01	-62.44	0.82 ^c

^a Free energy relative to the global minimum for each cluster of conformers, expressed in kcal mol⁻¹; see Methods section for the details of the QM calculation.

^b Expressed in degrees (see Fig. 4 for the definition of ϕ and ψ).

^c RMSD from the crystallographic coordinates of **4a**, calculated in Å over all heavy atoms.

298.15 K) and G^{solv} (solvation free energy, calculated by the C-PCM method).


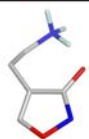

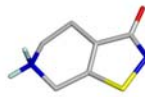

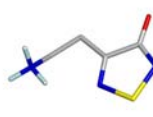
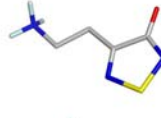
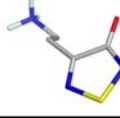
$$G_{aq}^{tot} = E^{ele} + E^{zp} + G^{therm} + G^{solv} \quad (1)$$

The results have been reported as the difference in free energy between each conformer and the global minimum.

On compounds **2**, **3** the first step was not performed by an *ab initio* systematic torsional scan, since the number of conformers (6912 and 165888 enantiomeric pairs, respectively) would have been computationally untreatable with QM *ab initio* methods. A stochastic search was instead accomplished with the StochasticCSearch module implemented in MOE, using the MMFF94s force field. Solvent effects were modelled according to the generalised Born/surface area (GB/SA) approach, setting the dielectric constants for the molecule and bulk water to 1 and 80, respectively, with no cutoff for non-bonded interactions;

atom-centred charges were fit to the *ab initio* electrostatic potential through the RESP procedure [18]. Each conformer was minimised until the RMS gradient was lower than 1·10⁻³ kcal mol⁻¹. Conformations were rejected if the RMS deviation from already existing ones was lower than 0.5 Å, or if their energy was more than 7 kcal above the global minimum. A maximum of 10⁴ iterations were performed on each molecule, and the search was abandoned after 1000 consecutive failures to find a new conformer. The search was repeated 10 times to make sure that all low energy conformers had been found. After choosing one enantiomer from enantiomeric conformer pairs, 9 conformers were identified for compound **2**, 21 for compound **3**. These conformations underwent full *ab initio* geometry optimisation with a 1·10⁻⁵ Hartree Bohr⁻¹ convergence criterion, and were then characterised as true minima by means of vibrational analysis as previously described. The conformations exceeding a 5-kcal threshold from the global

Table 4 Stable conformers of hypothesised models **14**, **15** (ab initio C-PCM systematic search)

	Conformer	ΔG^a	ϕ^b	ψ^b	RMSD
THIP 4a		-	161.91	45.55	0.00 ^c
Model 14		0.00	56.96	-74.48	1.33 ^c
		+4.68	-69.20	-63.16	0.80 ^c
Thio-THIP 4b		-	162.84	45.93	0.00 ^d
Model 15		0.00	60.36	-80.11	1.28 ^d
		+1.67	169.56	63.11	0.19 ^d
		+2.68	-179.04	-179.32	0.73 ^d
		+3.49	72.44	-179.45	0.99 ^d

^a Free energy relative to the global minimum for each cluster of conformers, expressed in kcal mol⁻¹; see Methods section for the details of the QM calculation.

^b Expressed in degrees (see Fig. 4 for the definition of ϕ and ψ).

^c RMSD from the crystallographic coordinates of **4a**, calculated in Å over all heavy atoms.

^d RMSD from the crystallographic coordinates of **4b**, calculated in Å over all heavy atoms.

minimum were discarded; the remaining ones are listed in Table 5.

On compounds **1–3**, **12**, **14**, **15** another conformational search through molecular dynamics (MD) was carried out, modelling the solvent explicitly. To this purpose, a random starting conformer was soaked in a cubic water box with a 30.28 Å side using the water soak facility implemented in MOE; the ligand and water coordinates were then imported into CHARMM [19]. The MMFF parameters were used throughout the simulations along with the MMFF-specific *vtrunc* method of evaluating non-bonded interactions. Particle mesh Ewald periodic boundary conditions were chosen (dielectric constant = 1.0), setting *cutim*, *ctvtrn*,

cutnb, *ctonnb*, *ctofnb* cutoff parameters to 14.0, 12.0, 14.0, 10.0 and 12.0 Å, respectively. Non-bonded and image lists were updated when necessary (heuristic test). Before MD, starting coordinates were minimised with a loose convergence criterion of 0.01 kcal mol⁻¹ Å⁻¹ according to the adopted basis Newton-Raphson method in three steps: firstly, the solute coordinates were restrained with a harmonic constraint of 1.0 kcal mol⁻¹ Å⁻²; then, the constraint was removed from the solute and put on water molecules; finally, all constraints were removed and full relaxation was allowed. Molecular dynamics were carried out constraining all bonds involving hydrogen with the SHAKE algorithm. Firstly, the system was gradually heated

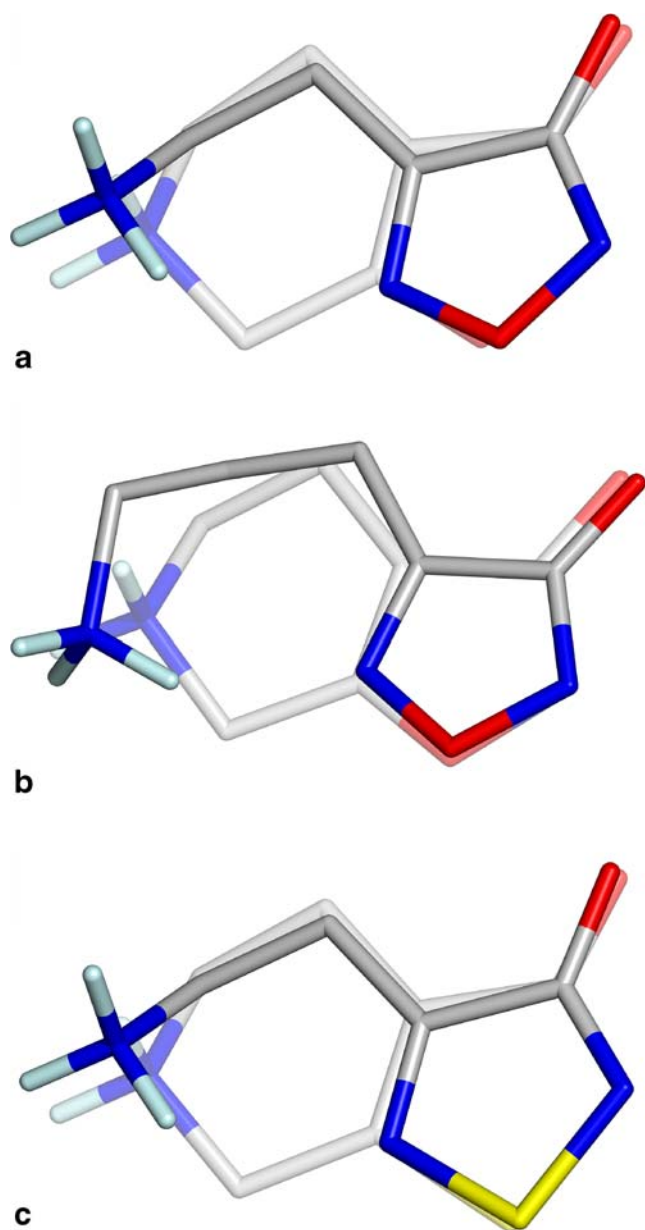


Fig. 5 Superposition between: a, b) the putative bioactive conformer of **1**, **2** (light colours) and the crystallographic conformation of **4a** (intense colours, RMSD=0.23, 0.27 respectively); c) the putative bioactive conformer of **15** (light colours) and the crystallographic conformation of **4b** (intense colours, RMSD=0.19). Non-polar hydrogens have been omitted for clarity. This figure, as well as the ones embedded in Tables 3, 4, 5, 6 and 7, 8, 9, 10, 11 (Electronic supplementary material), was realised with PyMOL [25]

at constant pressure from 0 to 300 K over 50ps (time step 0.2 fs), constraining all atoms with a force constant of $5.0 \text{ kcal mol}^{-1} \text{ \AA}^{-2}$. Then, the constraint was reduced to $1.0 \text{ kcal mol}^{-1} \text{ \AA}^{-2}$ and 50 ps of constant pressure dynamics at a constant temperature of 300 K were run (time step 0.5 fs, Hoover algorithm). Further 50 ps of constant p/T equilibration (time step 1.0 fs) with no constraints were carried out in order to let the system achieve the correct

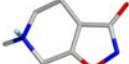









density. Afterwards, constant V/T conditions were chosen (time step 1.0 fs, Nosé-Hoover algorithm), setting the periodic box size as the average size during the last 25 ps of the previous constant p/T equilibration trajectory. After a 50-ps equilibration run, a production run of 1 ns was accomplished, using the multi-heat bath method as implemented in CHARMM: while bulk water was kept at 300 K, the solute was coupled with a 600 K heat bath, in order to overcome easily rotational barriers and achieve thorough conformational sampling. The 200 conformers were extracted from the trajectory at 5-ps intervals; since large deviations from equilibrium geometries are to be expected running MD at high temperature, all solvated conformers were minimised according to the procedure described previously, but with a tighter convergence criterion of $1.0 \cdot 10^{-4} \text{ kcal mol}^{-1} \text{ \AA}^{-1}$. Water molecules were stripped off the 200 minimised snapshots and a molecular database was built in MOE out of the naked solute conformers. Duplicate conformers (heavy-atom RMSD threshold = 0.2 Å) and mirror images were removed, then on the remaining geometries a potential energy evaluation was carried out with the GB/SA method as implemented in MOE, as previously described. The whole MD process was repeated five times starting from different random conformations; for all compounds the results were almost identical over the five runs and are reported in Table 6 for compound **1**. Data concerning compounds **2**, **3**, **12**, **14**, **15** can be found in the Electronic supplementary material (Tables 7, 8, 9, 10, 11).

The isodensity surfaces represented in Fig. 6 were generated with MOLDEN [20] from GAMESS output files. The electron density was evaluated on an evenly spaced cubic grid with a 20 Å side and a 0.2 Å mesh, then contoured at $0.07 e \text{ Bohr}^{-3}$ level. The electrostatic potential was evaluated on the same points as the electron density and colour-mapped on the isodensity surface. All calculations were run on a Linux cluster composed of 24 CPUs (Pentium IV single core, clock frequency ranging from 1.6 to 3.2 GHz).

Results and discussion

In order to substantiate with theoretical data our claim of bioisosterism between the hydroxyfurazanyl moiety and the carboxyl group, we calculated structural and electronic features of furazan-3-ol **16** with *ab initio* methods, extending the analysis also to its isoxazol congener **18**. As a representative planar molecule containing the carboxyl group, acrylic acid **17** was chosen (Table 2). Since both crystallographic and theoretical data are available for **18** [21], the same levels of theory chosen by Frydenvang and co-workers were used to allow results comparison. Both dipole moments and CHELPG ESP charges reported in [21]

Table 5 Stable conformers of compounds **2**, **3** (MM GB/SA stochastic search)

	Conformer	ΔG^a	ϕ^b	ψ^b	RMSD
THIP 4a		-	161.91	45.55	0.00 ^c
Compd 2		0.00	84.41	-54.30	1.41 ^c
		+1.95	-69.74	-67.37	1.00 ^c
		+2.42	170.71	68.17	0.27 ^c
		+4.29	70.20	59.54	0.63 ^c
Compd 3		0.00	-64.33	142.99	1.61 ^c
		+0.16	87.20	-55.95	1.52 ^c
		+0.99	74.09	-177.41	1.63 ^c
		+2.14	-69.82	-67.00	1.14 ^c
		+4.15	178.48	88.24	0.38 ^c

^a Free energy relative to the global minimum for each cluster of conformers, expressed in kcal mol⁻¹; see Methods section for the details of the QM calculation.







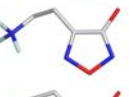
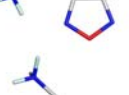


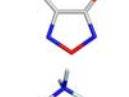
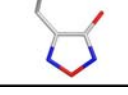
^b Expressed in degrees (see Fig. 4 for the definition of ϕ and ψ).

^c RMSD from the crystallographic coordinates of **4a**, calculated in Å over the ring atoms and the charged terminals.

for **18** could be almost exactly reproduced at the HF/6–31G(d) level, while small differences were noticed at the MP2/6–311G(d,p) level, probably connected with different convergence criteria in SCF iterations and geometry

optimisations. Only MP2/6–311G(d,p) data will be discussed for simplicity, since they were found to mimic more closely crystallographic geometries [21]; HF/6–31G(d) data are reported in the Electronic supplementary material

Table 6 Stable conformers of compound **1** (explicit solvent MD search)

	Conformer	ΔG^a	ϕ^b	ψ^b	RMSD
THIP 4a		-	161.91	45.55	0.00 ^c
Compd 1		0.00	-87.36	179.95	0.98
		0.45	-119.40	-178.47	0.85
		0.87	-71.84	-72.39	0.76
		1.02	-106.58	68.57	0.91
		1.17	-88.97	82.59	1.08
		1.46	129.47	81.10	0.32
		1.52	166.23	74.51	0.26
		1.79	-53.58	-175.18	1.09
		1.95	-161.38	61.69	0.41
		2.35	-67.56	79.61	1.24
		3.07	-46.10	78.11	1.34

^a Free energy relative to the global minimum for each cluster of conformers, expressed in kcal mol⁻¹; ΔG values were calculated with a MM GB/SA method (see Methods section for details).

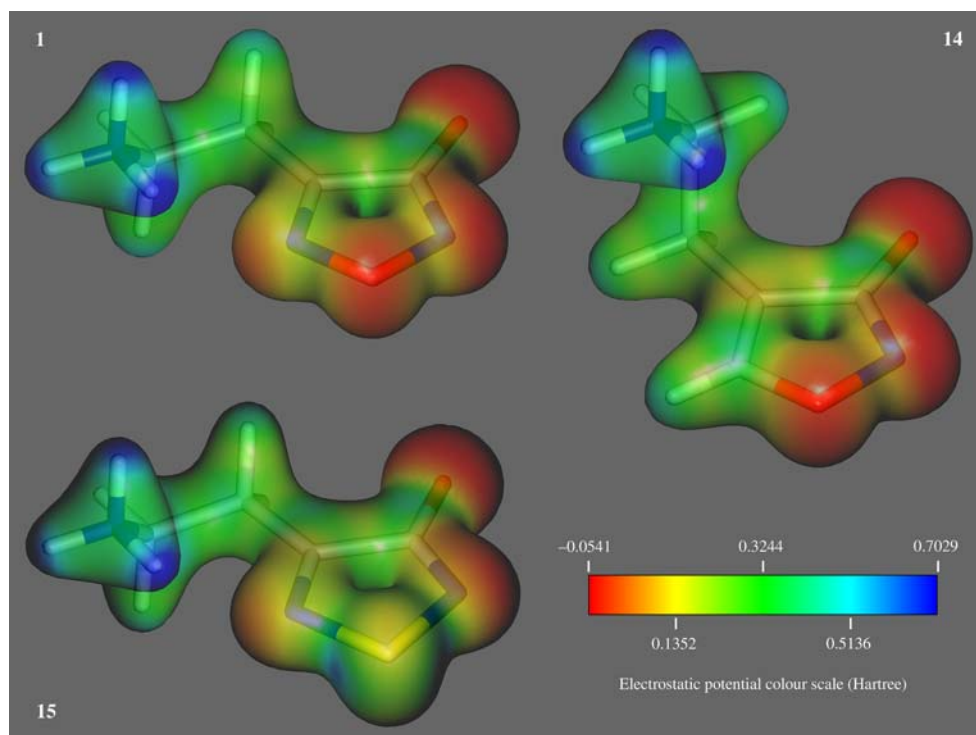
^b Expressed in degrees (see Fig. 4 for the definition of ϕ and ψ).

^c RMSD from the crystallographic coordinates of **4a**, calculated in Å over all heavy atoms.

(Table 2a). The hydroxyfurazanyl moiety displays acidic properties: 4-propylfurazan-3-ol has a pK_a of 3.77, while the acidic pK_a for compounds **1–3** ranges from 3.12 to 3.56 [5]; the overall acidic character is somewhat more marked

than for isoxazol-3-ol ligands (THIP, $pK_a=4.4$; muscimol, $pK_a=4.8$ [14]), and is nearer to that of the carboxyl group in GABA ($pK_a=4.04$ [5]). Analysing the structural data reported in Table 2, a close resemblance in the geometry

Fig. 6 Electrostatic potential of **1**, **14**, **15** colour-coded on the isodensity surface (contoured at $0.07 e \text{ Bohr}^{-3}$). The electrostatic potential on the surface ranges from 0.1487 to 0.7975 Hartree; the colour scale has been chosen accordingly



of the H(1)-O(1)-C(1)-N(1) “carboxy-like” substructure between the furazan and isoxazol systems is evident (RMSD=0.018 Å); both substructures in **16** and **18** are highly superimposable with the corresponding atoms in **17** (RMSD=0.048 and 0.040 Å, respectively). The van der Waals volume of **16** (64.62 Å³) is a bit lower than that of **18** (72.75 Å³), due the smaller radius of nitrogen compared to carbon and to the absence of the H(3) hydrogen atom. When electronic features are compared, rather marked differences emerge between the furazan-3-ol on one side and the carboxylic and isoxazolic counterparts on the other. While the latter two share substantially the same electronic distribution on the H(1)-O(1)-C(1)-N(1) “carboxy-like” substructure, as evidenced by the values of ESP-derived charges and by the direction and intensity of the dipole moment vector, in the furazan-3-ol system the presence of an additional electronegative nitrogen induces a number of changes. While the hydroxyl bond is almost identical in the three systems, the C(1)-N(1) bond in **16** is less strongly polarised than in **18**, and therefore it mimics less closely the carbonyl bond of the carboxyl group. Even more importantly, the polarity of the C(2)-N(2) bond in **16** is reversed with respect to the corresponding C(2)-C(3) bond in **18**. While in the isoxazol-3-ol the C(3) atom is electropositive due to σ -withdrawal by the vicinal O(2) atom and to the increased charge on C(2) amenable to π -donation by O(2), in the furazan-3-ol the corresponding N(2) atom is characterised by a negative charge (−0.32), just a bit lower than the one on N(1) (−0.39); by contrast, the C(2) atom is mildly electropositive. The overall effect is that, compared

to **17** and **18**, the dipole moment in **16** is almost double in intensity and its direction is rotated leftwards by 58.6° and 77.1° respectively, pointing in the C(1)→O(2) direction. While for compounds **1–3** the different electronic distribution may impact negatively on the affinity of the H(1)-O(1)-C(1)-N(1) “carboxy-like” substructure for the receptor, it could impart a peculiar conformational profile to the aminoalkyl side chain. Since all pentatomic heterocycles showing agonist activity at the GABA_A receptor bearing a substituent in the position vicinal to the hydroxyl group are characterised by having the aminoalkyl sidechain constrained in a 6 or 7-term ring (e.g. compounds **4a b** and **8**, Fig. 2), we speculated that the bioactive conformation of compounds **1**, **2** could resemble that of their closed-ring congeners. It can be easily predicted that AEMI (**12**) can hardly assume a THIP-like conformation due to steric hindrance of the 5-methyl substituent, thus failing to activate the GABA_A receptor. To verify this hypothesis, we performed a systematic torsional scan on compounds **1**, **12** in order to explore their PES. Similarly to GABA, 4-(ω -aminoalkyl)-1,2,5-oxadiazol-3-ol and 4-(ω -aminoalkyl)-iso(oxa,thia)zol-3-ol derivatives exist predominantly as zwitterions at physiological pH [5, 10]. Since modelling multiply charged compounds with molecular mechanics (MM) can lead to overestimation of the electrostatic contribution, various strategies have been adopted. Larsen and co-workers carried out MM conformational searches (GB/SA model, MM3 force field) on the *N*-protonated form of 4-PIOL derivatives, treating the hydroxy group as unionised, since the oxyanion in its bioactive form is known to be hydrogen-bonded to an

arginine residue in the receptor [10]. Lorenzini and co-workers obtained good results performing a PM3 torsional scan on the zwitterionic molecules, modelling the solvent with an Onsager approach [23]. Since we were interested in a highly reliable estimation of electrostatics, which are likely to play a key role in the conformational preferences of the compounds under study, we decided to employ an *ab initio* RHF method, modelling water as a continuum with the C-PCM method [24]. We chose the 6–31G+(d) basis set as a good compromise between computational speed and accuracy; both polarisation and diffuse functions were included to properly account for the zwitterionic status of the molecules. In Fig. 4a, 4b the PES for compounds **1**, **12** is reported, as obtained from the first minimisation step (see Methods section); as already pointed out, the presence of a plane of symmetry is due to the fact that each conformer exists as an enantiomeric pair. Once the ranges of dihedrals ϕ , ψ giving rise to conformers in a 5-kcal energy span from the global minimum were identified, full unconstrained minimisation allowed to identify a few stable conformers, whose structures and energies relative to the global minimum are reported in Table 3. For both compounds the most stable conformation is the one in which a charge-enhanced hydrogen bond takes place between the oxyanion and the ammonium cation. However, for compound **1** the conformation nearest to the global minimum (+3.18 kcal) mimics very well the conformation of THIP determined by X-ray crystallography (Fig. 5a, heavy atom RMSD=0.23 Å).

This finding provides a sound explanation to the agonist activity of **1**, which however is 100-fold lower than that of THIP, since according to QM calculations the THIP-like bioactive conformation is not the most populated. Moreover, the loss of conformational degrees of freedom upon binding accounts for an unfavourable entropic contribution which is detrimental to the activity of the flexible compound **1** with respect to the rigid one **4a**. Finally, the inverted polarisation of the C(1)–N(1) bond (Table 2) may account for a lower affinity of the “carboxy-like” substructure for the receptor. Moving to compound **12**, in the conformation nearest to the global minimum (+3.54 kcal) the ammonium cation is forced to lie much farther from the isoxazole ring (heavy atom RMSD=0.82 from **4a**), due to the steric hindrance of the methyl group, while THIP-like conformations are not energetically accessible (Table 3).

Since such a result for compound **12** was largely expected, we wanted to elucidate if the THIP-like conformation assumed by **1** is just a consequence of the absence of hindering substituents in 5-position on the ring, or if it is amenable to the peculiar electronic features of the 1,2,5-oxadiazole system; if so, we were interested in knowing if the 1,2,5-thiadiazole analogue could eventually share such features. To this purpose, the 3D models of two structures were built, namely the 5-demethyl analogue of AEMI **14**

and the thiadiazole **15**, both of which are not known in the literature (Fig. 3). The same *ab initio* torsional scan was performed as for **1** and **12**; the results are shown in Fig. 4c, d and Table 4.

Again, the most stable conformers are the ones with facing charged groups. Compound **15** has a broader spectrum of available conformers, and the one nearest the global minimum (+1.67 kcal) is highly superimposable with the crystallographic coordinates of thio-THIP **4b** [13] (Fig. 5c, RMSD=0.19 Å). It is noteworthy that examining the PES of **14** the minima corresponding to the THIP-like conformations are much less shallow than in the PES of **1** and **15**, and their energy relative to the global minimum is well above the 5-kcal threshold. The conformation nearest to the global minimum (+4.68 kcal) is very similar to the one found for **12** (RMSD=0.80 from **4a**). This finding indicates that removing the steric hindrance represented by the methyl group in AEMI is not sufficient to stabilise a THIP-like conformation such as the one assumed by the oxadiazole analogue **1**. Therefore, the capability of assuming the bioactive conformation seems to be warranted by the peculiar electronic features of the 1,2,5-(oxa,thia) diazole systems with respect to the isoxazole ring. To further investigate this point, the electrostatic potential was calculated from the QM-derived wavefunction and mapped on the isodensity surface (Fig. 6). The negative electrostatic potential in correspondence of the nitrogen atom in 5-position on the 1,2,5-oxadiazole ring stabilises the THIP-like conformation, allowing a strong electrostatic interaction with the protonated amino group. On the contrary, the corresponding isoxazolic methine group gives rise to an almost neutral potential, so that THIP-like conformers are not energetically accessible. The negative potential on the nitrogen atom is present in the 1,2,5-thiadiazole ring too, in spite of the much lower electronegativity of the sulphur atom.

On the basis of these results, we wanted to verify if the lower activity of derivative **2** and the inactivity of **3** could be explained as well with their conformational preferences. Since the number of possible conformations is much higher due to the increased number of rotatable bonds, the PES torsional scan was accomplished by a stochastic MM search, then the conformations in a 5-kcal range from the global minimum underwent unconstrained optimisation by the same QM methods employed for the lower homologues. The results are reported in Table 5.

Once more, for compound **2** the global minimum is represented by a conformer in which the ionised groups interact closely. The nearest conformational minimum (+1.95 kcal) is characterised by an extended conformation of the 3-aminopropyl chain. At 2.42 kcal above the global minimum a conformer is found which is fairly superimposable with **4a** (Fig. 5b, RMSD=0.27 Å, calculated over the ring atoms and the charged terminals, since the number

of side chain carbons differs). The less precise match with **4a**, the existence of a low-energy extended conformer and the more unfavourable entropic term due to the loss of an additional torsional degree of freedom upon binding account for the lower activity of **2** with respect to **1**. When compound **3** was examined, four conformers were found (the global minimum and the ones lying respectively 0.16, 0.99, 2.14 kcal above it) which are more stable than the putative THIP-like bioactive one (+4.15 kcal, RMSD=0.38 Å from **4a**, calculated over the ring atoms and the charged terminals); at the same time, the side chain is not long enough to hypothesise a binding mode similar to that of 4-PIOL **5a** [10]. Therefore, the very low probability of assuming the bioactive conformation together with the increased molecular volume and an absolutely unfavourable entropic contribution account for the lack of activity of compound **3**.

Gálvez-Ruano and co-workers noticed that intramolecular interactions between oppositely charged groups in GABA_A ligands can be overestimated by implicit solvent models [26]. To check this possibility, we performed another conformational search through molecular dynamics, this time modelling solvent explicitly (see Methods for details). The potential energies of the solvated conformers thus obtained are too dependent on the bulk water coordinates, and therefore are not easily comparable; careful solvent sampling and energy averaging over a large number of configurations should be carried out to get reliable figures. Such a task would have been very time-consuming and not really necessary for our purposes; instead, we decided to rank the conformers according to their potential energy calculated with the GB/SA approach, after stripping off the water molecules. The results for compound **1** are reported in Table 6.

A larger number of stable conformers were found with this kind of search, since the presence of the solvent molecules complicates the PES allowing the existence of more local minima. The relative energy ranking is actually inverted with respect to the one found by the QM systematic search, with the most stable conformers being the ones with the side chain in an extended configuration, and the least stable those with charged groups facing each other. However, also in this case two THIP-like conformers are found in the middle (heavy-atom RMSD 0.26 and 0.32 from THIP, respectively), with almost identical geometries with respect to the one found by QM methods; their energy relative to the global minimum is about +1.5 kcal, so the validity of the discussion made previously is confirmed. Tables 7, 8, 9, 10, 11 (Electronic supplementary material) report all conformations for compounds **2**, **3**, **12**, **14**, **15**. Also in the case of compound **2**, the extended conformers are energetically more favourable than the ones with facing charged groups, but again two THIP-like conformers are found

(RMSD=0.22, E=+2.06 kcal; RMSD=0.40, E=+0.76 kcal) as in the MM GB/SA stochastic search. In the case of compound **3** the results justify even more the feeble affinity for the receptor, since no THIP-like conformers are found, but only many conformers with the side chain in an extended configuration. For both isoxazolic models **12**, **14**, the same picture as in the QM search was found, with no THIP-like conformers and folded conformers more stable than the extended ones. Moving to the thiadiazolic model **15**, again a THIP-like conformer can be recognised (RMSD=0.49, E=+1.25 kcal), together with mixed folded and extended conformers with energies between the global minimum and +1.08 kcal. On the whole, the MD search in explicit solvent validated the results obtained with the QM C-PCM method and the MM stochastic search about the distinct conformational preferences of (oxa,thia)diazolic ligands compared to the isoxazolic analogues **12**, **14**. Implicit solvent models, both QM and MM, confirm their tendency towards overestimating intramolecular electrostatic interactions when dealing with zwitterionic molecules.

Summary

Geometric and electronic features of the 1,2,5-oxadiazol-3-ol ring system have been analysed with theoretical methods and compared with the carboxy group as well as with its isoxazol counterpart, in order to demonstrate non-classical isosterism. While acidity and geometries are quite comparable, the electronic distribution displays rather marked differences. A conformational study has been carried out to elucidate the putative bioactive conformation of compounds **1**, **2**, which are the only examples of pentatomic heterocycles bearing a flexible side chain in the position vicinal to the hydroxyl group displaying agonist activity at the GABA_A receptor. For both of them, an energetically accessible conformer has been identified which closely mimics the crystallographic conformation of THIP. The same conformer is not energetically accessible for the isoxazole analogues **12**, **14**, while appears to be available to the 1,2,5-thiadiazole analogue **15**. The reason of the conformational profile shown by the 1,2,5-(oxa,thia)diazole derivatives seems to rely largely in the electrostatic potential at the nitrogen atom in position 5 on the ring. Compound **4b**, the sulphur analogue of THIP, was found to be 300 times less active than **4a**; a steric clash between the bulkier sulphur atom and the receptor has been invoked to explain this behaviour [6]. The synthesis and pharmacological characterisation of **15** would allow to verify if the same picture holds true or if the greater flexibility of the side chain allows it to avoid the aforementioned steric clash, and possibly display higher affinity than **1** due to the increase in hydrophobicity, as in the case of **5b** with respect

to **5a** [6], and to the higher propensity to assume the bioactive conformation (only 1.67 kcal above the global minimum instead of 3.18). The conformational analysis allowed rationalising the lower activity of **2** and the inactivity of **3** as well. Therefore, ω -aminopropyl-1,2,5-oxadiazolols **1**, **2** have proved to possess a distinct conformational profile with respect to the isoxazolol analogues, which confers them affinity for the GABA_A receptor. The elucidation of the electronic properties of 1,2,5-oxadiazolols can prove useful in the design of new ligands employing this ring system as a bioisoster of the carboxy group.

Acknowledgements The research reported here was supported by a MIUR grant (COFIN 2005). This work is dedicated to Prof. Alberto Gasco (University of Turin), who introduced us to the chemistry of the 1,2,5-oxadiazole system. We wish to thank an anonymous referee for his helpful suggestions.

References

- Patani GA, LaVoie EJ (1996) *Chem Rev* 96:3147–3176. DOI 10.1021/cr950066q
- Thornber CW (1979) *Chem Soc Rev* 8:563–580. DOI 10.1039/CS9790800563
- Burger A (1991) *Prog Drug Res* 37:287–371
- Lolli ML, Giordano C, Nielsen B, Johansen TN, Fruttero R, Gasco A (2006) Proc 232nd ACS National Meeting San Francisco, CA, USA, 10–14 Sept Abstracts (MEDI 520)
- Lolli ML, Hansen SL, Rolando B, Nielsen B, Wellendorph P, Madsen K, Larsen OM, Kristiansen U, Fruttero R, Gasco A, Johansen T (2006) *J Med Chem* 49:4442–4446. DOI 10.1021/jm051288b
- Krehan D, Storustovu Si, Liljefors T, Ebert B, Nielsen B, Krogsgaard-Larsen P, Frølund B (2006) *J Med Chem* 49:1388–1396. DOI 10.1021/jm050987l
- Krogsgaard-Larsen P, Honoré T, Hansen JJ, Curtis DR, Lodge D (1981) *Adv Biochem Psychopharmacol* 27:285–294
- Krehan D, Frølund B, Ebert B, Nielsen B, Krogsgaard-Larsen P, Johnston GAR, Chebib M (2003) *Bioorg Med Chem* 11:4891–4896. DOI 10.1016/j.bmc.2003.09.016
- Hoeg S, Greenwood JR, Madsen KB, Larsson OM, Frølund B, Schousboe A, Krogsgaard-Larsen P, Clausen RP (2006) *Curr Top Med Chem* 17:1861–1882. DOI 10.2174/156802606778249801
- Frølund B, Jørgensen AT, Tagmose L, Stensbøl TB, Vestergaard HT, Engblom C, Kristiansen U, Sanchez C, Krogsgaard-Larsen P, Liljefors T (2002) *J Med Chem* 45:2454–2468. DOI 10.1021/jm020027o
- Molecular Operating Environment 2006.08 (MOE), Chemical Computing Group Inc., Montreal, Quebec, Canada; <http://www.chemcomp.com>
- GAMESS-US version 24 Mar 2007, Iowa State University, Ames, IA; Schmidt MW, Baldrige KK, Boatz JA, Elbert ST, Gordon MS, Jensen JH, Koseki S, Matsunaga N, Nguyen KA, Su SJ, Windus TL, Dupuis M, Montgomery JA (1993) *J Comput Chem* 14:1347–1363. DOI 10.1002/jcc.540141112
- Lipkowitz KB, Gilardi RD (1989) *J Mol Struct* 195:65–77. DOI 10.1016/0022-2860(89)80159-0
- Brehm L, Ebert B, Kristiansen U, Wafford KA, Kemp JA, Krogsgaard-Larsen P (1997) *Eur J Med Chem* 32:357–363. DOI 10.1016/S0223-5234(97)89089-7
- Barone V, Cossi M (1998) *J Phys Chem A* 102:1995–2001. DOI 10.1021/jp9716997
- Cossi M, Rega N, Scalmani G, Barone V (2003) *J Comput Chem* 24:669–681. DOI 10.1002/jcc.10189
- Scott AP, Radom L (1996) *J Phys Chem* 100:16502–16513. DOI 10.1021/jp960976r
- AMBER version 9, TSRI, La Jolla, CA, USA; Wang J, Cieplak P, Kollman PA (2000) *J Comput Chem* 21:1049–1074. DOI 10.1002/1096-987X(200009)21:12<1049::AID-JCC3>3.0.CO;2-F
- CHARMM version c33b1, Harvard University, Cambridge, MA, USA; Brooks BR, Bruccoleri RE, Olafson BD, States DJ, Swaminathan S, Karplus M (1983) *J Comput Chem* 4: 187–217. DOI 10.1002/jcc.540040211
- MOLDEN version 4.6, CMBI, the Netherlands; Schaftenaar G, Noordik JH (2000) *J Comput Aid Mol Des* 14:123–134. DOI 10.1023/A:1008193805436
- Frydenvang K, Matzen L, Norrby PO, Sløk FA, Liljefors T, Krogsgaard-Larsen P, Jaroszewski JW (1997) *J Chem Soc Perkin Trans 2*:1783–1791. DOI 10.1039/a700332c
- Allouche AR, Gabedit version 2.1.0; <http://gabedit.sourceforge.net>.
- Lorenzini ML, Bruno-Blanch L, Estiù GL (1998) *J Mol Struct (THEOCHEM)* 454:1–16. DOI 10.1016/S0166-1280(98)00138-9
- Tomasi J, Persico M (1994) *Chem Rev* 94:2027–2094. DOI 10.1021/cr00031a013
- DeLano WL, The PyMOL Molecular Graphics System, DeLano Scientific, Palo Alto, CA, USA; <http://pymol.sourceforge.net>.
- Gálvez-Ruano E, Iriepa I, Morreale A, Boyd DB (2001) *J Mol Graph Model* 20:183–197. DOI 10.1016/S1093-3263(00)00081-4